Academic Research Publishing Group


**Scientific Review**
**ISSN(e): 2412-2599, ISSN(p): 2413-8835**
**Vol. 2, No. 3, pp: 35-52, 2016**
**URL:** http://arpgweb.com/?ic=journal&journal=10&info=aims

# Heterogeneous Performance Evaluation of Sophisticated Versions of CFAR Detection Schemes

**Mohamed B. El Mashade** Electrical Engineering Dept., Faculty of Engineering, Al Azhar University, Nasr City, Cairo, Egypt

**Abstract:** The detection of radar targets in a background, the statistical parameters of which are unknown and may not be stationary, can be effectively achieved through CFAR processors. The CA-CFAR scheme performs optimally for homogeneous and exponentially distributed clutter observations. However, it exhibits severe performance degradation in the presence of outlying target returns in the reference set or in regions of abrupt change in the background clutter power. The OS-CFAR processor has been proposed to alleviate both of these problems. Although this processor may treat target multiplicity quite well, it lacks effectiveness in preventing excessive false alarms during clutter power transitions. The TM-CFAR algorithm, which implements trimmed averaging after ordering, can be considered as a modified version of OS technique. By knowingly excising the ordered samples, the TM detector may actually perform somewhat better than the OS processor. To simultaneously exploit the merits of CA, OS, and TM schemes, two combinations namely CA_OS and CA_TM have been recently suggested. Each one of these versions optimizes good features of two CFAR detectors depending on the characteristics of clutter and searched targets with the goal of enhancing the detection performance under constant level of false alarm. It is realized by parallel operation of two standard types of CFAR schemes. Our goal in this paper is to analyze these two developed versions, in heterogeneous situations, to show to what extent they can improve the behavior of the conventional CFAR processors.

**Keywords:** CFAR detection; clutter edges; Spurious targets; Fluctuating targets; Receiver operating characteristics (ROC's); Signal-to-noise ratio (SNR) loss.

## 1. Introduction

Radar is an invention that can be considered as an addition to man's sensory equipment which affords genuinely new facilities. It enables a certain class of objects to be seen, that is detected and located, at distances far beyond those at which they could be distinguished by the unaided eye. This seeing is unimpaired by night, fog, cloud, smoke, and most other obstacles to ordinary vision. Additionally, radar permits the measurement of the range of the objects it sees with a convenience and precision entirely unknown in the past. Furthermore, it can measure the instantaneous speed of such an object toward or away from the observing station in a simple and natural way. The superiority of radar to ordinary vision lies in the greater distances at which seeing is possible, in its ability of working regardless of light condition and of obscuration of the object being seen, and in the unparalleled ease with which target range and its rate of change can be measured [1-5].

Detection of targets represents one of the most fundamental tasks of a radar system. This task is associated with the process of examining the radar data to see if it is regarded as interference only, or interference plus echoes from a target of interest. Once a target is detected, the system can turn its attention to processing the target information. Depending on the type of radar application, the system might be concerned with estimating the target radar cross section (RCS), measuring and tracking its position or velocity, imaging it, or providing fire control data to direct weapons to the target.

From the detection point of view, radars are increasingly required to detect small targets in the presence of strong clutter while simultaneously maintaining a low, and preferably constant, level of false alarm. Two key radar subsystems for achieving this goal are the Doppler filter, for suppressing clutter as far as possible, and the automatic detector, for deciding which of the filtered returns represent targets. Since the false alarm rate is very sensitive to the setting of the detection threshold, changes in radar characteristics with time (ageing) and changes in the target background characteristics mean that a fixed detection threshold is not practical. Additionally, the operational environments of radar systems have different sources of noise that deteriorate their performance. Moreover, thermal noise generated by the radar itself is unavoidable. Furthermore, returns from other targets referred to as interfering targets, unwanted echoes (clutter) typically from the ground, sea, rain or other participation, chaff and small objects, interfere with the detection of the desired targets. Therefore, it is of safety to employ such type of detectors which has a feature that automatically adjusts its sensitivity according to variety of the interference power in order to maintain a constant rate of false alarm irrespective of the circumstances. Detector in radar receivers with this feature is known as constant false alarm rate (CFAR) processor [6-10].

Modern radar systems perform this detection automatically in the signal/data processor. It is accomplished by establishing a threshold signal level (voltage) on the basis of the current interference (e.g., external noise, clutter, internal receiver thermal noise) voltage and then by deciding on the presence of a target by comparing the signal level in every cell with that threshold. If the signal level exceeds the threshold, then the presence of a target is declared whilst no target is proclaimed if the threshold surpasses the signal strength. However, in a clutter environment with large clutter spikes, the clutter will occasionally cross the threshold and falsely be declared as targets. Therefore, the objective of the threshold is to detect targets in addition to minimizing the number of false alarms. Ideally, all targets should be detected and no false alarms should occur. Increasing the threshold will reduce the probability of falsely detecting clutter reflections, but it also reduces the probability of detecting targets that reflect small amounts of signal energy compared to the clutter. As it is desired to detect as many targets as possible, the threshold often needs to be set at a level where false alarms are unavoidable. Thus, higher detectability is achieved on the expense of higher false alarm rate. To find suitable threshold values, a common approach is to try to control the probability of false alarms. In practice, the clutter environment might change over time and the knowledge of all possible clutter values is difficult to obtain. Thus, it may be more tractable to adapt the threshold to the current clutter environment and obtain a local $P_{fa}$. If a local $P_{fa}$ is maintained by adjusting the threshold, the overall $P_{fa}$ will also be maintained. In most cases, setting an adaptive threshold involves measuring the local clutter mean level [11].

The threshold set by the CFAR technique is obtained on a sample by sample basis, using estimated noise power by processing a group of samples surrounding the sample under investigation**.** Several variants of the CFAR algorithm have been proposed in the radar literature to deal with different problems excited in radar applications. These techniques require linear operations (such as getting the maximum, minimum, or average of a set of values) or nonlinear operations like sorting a set of values and selecting one on a specific position before performing a linear operation. These different algorithms have been developed in order to increase the target detection probability under several environment conditions, especially to deal with two of them: regions of clutter transitions and multiple target situations. The first situation occurs when the total received noise power within a single reference window changes abruptly, leading to excessive false alarm or target masking. The second situation is encountered when there are two or more closely spaced targets in the reference cells, leading the CFAR processor to report only the strongest one of them, i.e., there is a target masking [12-15].

Some CFAR algorithms offer better performance than others where they provide greater probability of detection for a given value of signal-to-noise ratio (SNR), lower average decision threshold and as low as possible probability of false alarm deviations from the desired values. The CA scheme performs well in homogeneous situation whilst the ordered statistic based detector has good behavior against the presence of heterogeneity that may exist in the estimation channel. Our goal in this paper is to analyze the two modified combinations, namely CA_OS- and CA_TM-CFAR, in non-homogeneous situations and compare their performance with the original CFAR processors. The new CFAR procedures have some advantages over other types of CFAR detectors.

The rest of the paper is organized as follows. The model description that has been used to analyze the performance of the selected detectors is discussed in Section II. Section III is devoted to the heterogeneous analysis of the detectors under examination and exact expressions for their performances are derived. Homogeneous and non-homogeneous numerical results are presented in Section IV and our concluded remarks are outlined in Section V.

## 2. Processor Description and Statistical Background

In a CFAR processor, the square-law detected signal is sampled in range by the range resolution cells, and the resulting samples are stored in a tapped delay line as shown in Fig.(1). The output of the cell under test (CUT), which is the one in the middle of the tapped line, is denoted by Θ. The outputs of the surrounding cells are combined through a specified processing to yield an estimate $Z$ of the noise level in the tested cell which is then multiplied by a constant scale factor T imposed to achieve the desired rate of false alarm for a given size N of the reference window when the total background noise is homogeneous. The content of the CUT is compared with the adaptive threshold (ZT) to make a decision about the presence or the absence of a target in that cell. In other words, the problem of detecting signals (radar targets) in presence of interference (clutter and noise) can be formulated as a binary hypothesis test. In this test, the detector has to discern between two hypotheses: target is absent (null hypothesis: $H_0$) or target is present (alternative hypothesis: $H_1$). This decision is made from an observation vector obtained by the radar receiver. Mathematically, this decision can be formulated as:

$$\Theta \underset{H_0}{\overset{H_1}{\gtrless}} Z\,T \qquad (1)$$

The block diagram of typical CFAR procedure is shown in Fig.(1). The received i.f. signal is applied to a matched filter, the output of which is then passed through a square-law device to extract the baseband signal. This signal is then sampled and the sampling rate is chosen in such a way that the samples are statistically independent. The square-law detected video range samples are sent serially into a shift register of N+1 resolution cells. The content of the cell under test is the one in the middle of the processing window. The center bin (CUT) is tested on whether it contains a target's return or not. The detection procedures involve the comparison of the received signal with a certain threshold. The CFAR schemes set this threshold adaptively according to local information on the background noise power. The estimation of the mean power of the local clutter (Z) is usually based on the N neighboring bins. The name of the specific CFAR detector is determined according to the kind of operation used to estimate the unknown noise power level. Here, we are concerned with a parallel combination of the reference cells that are fed two estimators: one of them is based on the CA algorithm while the other follows the TM technique. Each estimated power is weighted by a constant scale factor T, which is chosen in such a way that the requested rate of false alarm can be achieved. Each one of the resulted statistics is separately compared with the content of the CUT to decide whether the received signal belongs to the searched target or it contains noise background. The obtained two decisions are combined to represent the inputs of an "AND" gate, the output of which is either low or high to represent the final decision about the absence or presence of the tested target, respectively. In other words, the finite decision about target presence is made in fusion center which is composed of one "AND" logic circuit. If the both input single decision in the fusion center are positive, the finite decision of the fusion center is presence of the target in cell under test. In each other cases, finite decision is negative and target is not at the location which corresponds to the CUT.

To start our problem formulation, let us suppose that the input signal to the receiver is composed of the radar echo signal s(t) and additive zero-mean white Gaussian noise $n(t)$ with variance $\sigma^2$. The input noise is assumed to be spatially incoherent and uncorrelated with the signal. The received i.f signal is applied to a matched filter which is specifically designed to maximize the output signal-to-noise ratio (SNR). The output of this filter is the signal $\Theta(t)$, which can be written as

$$\Theta(t) \triangleq \Theta_I(t)\cos(\omega_0 t) + \Theta_Q(t)\sin(\omega_0 t) = r(t)\cos(\omega_0 t - \theta(t)) \tag{2}$$

where $\omega_0 = 2\pi f_0$ is the radar operating frequency, $r(t)$ and $\theta(t)$ denote the envelope and phase, respectively, of $\Theta(t)$, and the subscripts $I$ & $Q$ refer to the inphase and quadrature components. A target is detected when $r(t)$ exceeds the threshold value $\Theta_T$, otherwise the received signal contains no target return.

If the filter output is a complex random variable (RV) that is composed of either noise alone or noise plus target signal return (sine wave of amplitude A), the quadrature components take the forms:

$$\Theta_L(t) \triangleq \begin{cases} A + n_L(t) & \text{in the presence of target return} \\ n_L(t) & \text{in the absence of target return} \end{cases} \qquad L = I, Q \tag{3}$$

The inphase and quadrature components of noise, $n_I(t)$ and $n_Q(t)$, are uncorrelated zero-mean low pass Gaussian noise with equal variances $\sigma^2$. The joint probability density function (PDF) of them is given by:

$$\begin{aligned} f(n_I, n_Q) &= \frac{1}{2\pi\sigma^2} \exp\left(-\frac{n_I^2 + n_Q^2}{2\sigma^2}\right) \\ &= \frac{1}{2\pi\sigma^2} \exp\left(-\frac{(r\cos\theta - A)^2 + (r\sin\theta)^2}{2\sigma^2}\right) \end{aligned} \tag{4}$$

In terms of the joint probability density function of $n_I(t)$ and $n_Q(t)$, we can evaluate the joint PDF of the new random variables $r(t)$ and $\theta(t)$ as

$$f(r, \theta) = \frac{r}{2\pi\sigma^2} \exp\left(-\frac{r^2 + A^2}{2\sigma^2}\right) \exp\left(\frac{rA\cos\theta}{\sigma^2}\right) \tag{5}$$

The PDF of $r$ is obtained by integrating Eq.(5) over $\theta$. Thus,

$$f(r) = \frac{r}{\sigma^2} \exp\left(-\frac{r^2 + A^2}{2\sigma^2}\right) I_0\left(\frac{r A}{\sigma^2}\right) \tag{6}$$

In the above mathematical expression, $I_0(.)$ denotes the modified Bessel function of order 0. In the literature, the above PDF is known as Rice distribution. It is obvious that in the absence of radar target return ($A$ = 0), this distribution tends to Rayleigh PDF. On the other hand, if ($rA/\sigma^2$) becomes very large, Eq.(6) tends to Gaussian PDF with mean A and variance $\sigma^2$ [9].

When a target is illuminated by the radar beam, it normally reflects numerous pulses. The radar detection probability is enhanced by summing all (or most) of the returned pulses. The process of adding radar echoes from many pulses is known as pulse integration. This process can be performed on the quadrature components prior to or after the envelope detector. The pulse integration in the first case is called coherent or pre-detection while in the second case, it is known as non-coherent or post-detection integration. Coherent integration preserves the phase relationship between the received pulses and consequently, a build up in the signal amplitude is achieved. In post-detection integration, on the other hand, the phase relation is destroyed. In coherent integration of $M$ pulses, it is shown that the signal power is unchanged, while the noise power is reduced by a factor of $1/M$. Therefore, the SNR in the process of coherent integration of $M$ pulses is improved by $M$. However, the requirement of reserving the phase of each transmitted pulse as well as maintaining coherency during propagation is very costly and challenging to achieve. For these reasons, most radar systems prefer non-coherent integration owing to its ease of implementation. Therefore, let us now go to calculate the PDF of non–coherently integrated M pulses.

The output of the square-law detector for the $\ell$th pulse is proportional to the square of its input. Thus, it is convenient to define new variables as

$$\vartheta_\ell \triangleq \frac{r_\ell^2}{2\sigma^2} = \frac{r_\ell^2}{\psi} \quad , \quad \Lambda \triangleq \frac{A^2}{\psi} \quad \& \quad \psi = 2\sigma^2 \tag{7}$$

The PDF of the variable at the output of the square-law detector is

$$f_{\vartheta_\ell}(\beta) = \exp[-(\beta + \Lambda)] \; I_0\left(2\sqrt{\beta\Lambda}\right) \tag{8}$$

Post-detection integration of $M$ pulses is implemented as

$$\Theta = \sum_{\ell=1}^{M} \vartheta_\ell \tag{9}$$

Since the RV's $r_i$'s are statistically independent, the PDF of $\Theta$ becomes

$$f_\Theta(\beta/\theta) = \left(\frac{\beta}{\theta}\right)^{\frac{M-1}{2}} \exp[-(\beta + \theta)] \; I_{M-1}\left(2\sqrt{\beta\theta}\right) \tag{10}$$

$I_{M-1}(.)$ denoted the modified Bessel function of order $M-1$. The parameter θ is the total, $M$ pulse, SNR; $\theta = M\Lambda$ in terms of per pulse SNR (Λ).

To model the target fading, the total SNR (θ) is taken to be random with prior PDF of $\chi^2$-distribution with $\kappa$-degrees of freedom. Thus,

$$f\left(\theta/\bar{\theta}\right) = \left(\kappa/\bar{\theta}\right)^\kappa \frac{\theta^{\kappa-1}}{\Gamma(\kappa)} e^{-\kappa\theta/\bar{\theta}} \; U(\theta) \tag{11}$$

In the above expression, $\bar{\theta}$ is the average M-pulse SNR, Γ(.) is the gamma function, and $U$(.) denotes the unit step function. In this model, any value of $\kappa > 0$ is acceptable. This model takes into account the correlation between non-coherent pulse bursts. In any event, the resulting primary target PDF for $\chi^2$ fluctuating target with $\kappa$-degrees of freedom is given by [13]

$$\begin{aligned} f_\Theta\left(\beta/\bar{\theta}\right) &= \int_0^\infty f_\Theta(\beta/\theta)\, f\left(\theta/\bar{\theta}\right) d\theta \\ &= \left(\frac{\kappa}{\bar{\theta}+\kappa}\right)^\kappa \frac{\beta^{M-1}}{\Gamma(M)} \, {}_1F_1\left(\kappa, M; \frac{\bar{\theta}}{\bar{\theta}+\kappa}\right) e^{-\beta} \end{aligned} \tag{12}$$

${}_1F_1(.)$ is the confluent hyper-geometric function. The characteristic function (CF) associated with Eq.(12) can be obtained by taking the Laplace transformation of it which results in

$$\Omega_\Theta(\omega) = \left(\frac{1}{\omega+1}\right)^{M-\kappa}\left(\frac{\varepsilon}{\omega+\varepsilon}\right)^{\kappa} \qquad \& \qquad \varepsilon \triangleq 1-\frac{\bar{\theta}}{\kappa+\bar{\theta}} \tag{13}$$

In the case where $\kappa = M$, the above formula tends to the well-known Swerling II (SWII) target fluctuation model. Therefore, when the target fluctuates in accordance with SWII model, its associated CF has a form given by

$$\Omega_\Theta(\omega)\Big|_{\kappa=M} = \left(\frac{\gamma}{\omega+\gamma}\right)^{M} \qquad \& \qquad \gamma \triangleq \frac{M}{\bar{\theta}+M} = \frac{1}{1+S} \tag{14}$$

In the above expression, S symbolizes the SNR per pulse. The Laplace inverse of the previous equation gives the PDF of the SWII target fluctuation model. Thus,

$$f_\Theta(x) = \left(\frac{1}{1+S}\right)^{M}\frac{x^{M-1}}{\Gamma(M)}\exp\left(-\frac{x}{1+S}\right) U(x) \tag{15}$$

Generally, for mono-pulse case (M=1), the previous formula becomes

$$f_X(x) = \alpha \exp(-\alpha x) \; U(x) \tag{16}$$

where

$$\alpha \triangleq \begin{cases} \alpha_t = 1/\psi & \text{for clear background} \\ \alpha_c = \alpha_t/(1+C) & \text{for clutter return} \\ \alpha_s = \alpha_t/(1+S) & \text{for tested target return} \\ \alpha_0 = \alpha_t/(1+I) & \text{for outlier return} \end{cases} \tag{17}$$

The basic parameters used to evaluate the detection capabilities of a detector are the probabilities of detection ($P_D$) and false alarm ($P_{FA}$). The $P_D$ is defined as the probability of deciding that target is present when the received signal is coming from a target. The $P_{FA}$ is defined as the probability of deciding that target is present when the received signal is not coming from a target, i.e. comes from clutter and noise. Generally, $P_D$ has a mathematical form given by [2].

$$P_D = \omega \; \Psi_Z(\omega)\Big|_{\omega=T\alpha_S} \tag{18}$$

with

$$\Psi_Z(\omega) \triangleq L\{F_Z(x)\} \tag{19}$$

"L" denotes the operator of Laplace transformation and $F_Z(.)$ represents the cumulative distribution function (CDF) of the noise level estimate Z. In the absence of the tested target return, Eq.(18) becomes representing the false alarm rate which can be written as:

$$P_{FA} = \omega \; \Psi_Z(\omega)\Big|_{\omega=T\alpha_t} \tag{20}$$

## 3. Processor Performance Analysis

In this section, we analyze three of CFAR processors, namely the CA-, OS-, and TM-CFAR processors, for their performance in homogeneous backgrounds as well as in regions of clutter transitions and in multiple target environments, with the object of obtaining closed-form performance expressions in each case.

### a) Cell-Averaging (CA) Detector

One of the most important CFAR schemes is the CA processor which adaptively sets the threshold by estimating the mean level in a channel of $N$ range cells. This type of detection procedures is the optimum CFAR processor (maximizes detection probability) in a homogeneous background when the reference cells contain independent and identically distributed (IID) observations governed by an exponential distribution [14]. As the size of the reference channel increases, the detection probability approaches that of the optimum detector which is based on a fixed threshold. However, there are two major problems that require careful investigation in such a CFAR detection scheme. They are those excited by regions of clutter power transition and those presented by multiple target environments. The first case occurs when the total noise power received within a single reference set changes abruptly. The presence of such a clutter edge may result in severe performance degradation in an adaptive threshold scheme leading to excessive false alarms or serious target masking depending upon whether the cell under test is a sample from clutter background or from relatively clear background with target return, respectively. The second situation is encountered when there are two or more closely spaced targets in range. The outlying targets that appear in the reference channel along with the target under test (known as primary target) may raise the threshold unnecessarily. Often a CFAR detector only reports the stronger of the two targets.

The CA-CFAR procedure uses the maximum likelihood estimate of the noise power to set the adaptive threshold under the assumption that the underlying noise distribution is exponential and the noise samples are IID. The processor performance is significantly affected when the assumption of homogeneous reference window is violated. In the case of multiple targets the noise estimate includes the interfering signal power- leading to an unnecessary increase in overall threshold. This leads to serious degradation in detection probability [6]. When a clutter edge is present in the reference window with a target return in the test cell, severe masking of targets results due to increase in threshold.

In order to analyze the CFAR detection performance when the candidates of the reference set no longer contain radar returns from a homogeneous background, as in the case of clutter edges, the assumption of statistical independence of the reference cells is retained. Let us assume that the reference set contains R cells from clutter background with noise power $\alpha_c$, and N-R cells from clear background with noise power $\alpha_t$. Thus, the total noise power can be estimated as:

$$Z_{CA} = \sum_{i=1}^{R} X_i + \sum_{j=R+1}^{N} Y_j \triangleq X + Y \tag{21}$$

The random variable X denotes the clutter return whilst Y represents the clear background. X and Y have CF's given by:

$$\Omega_X(\omega) = \left(\frac{\alpha_c}{\omega + \alpha_c}\right)^R \quad \& \quad \Omega_Y(\omega) = \left(\frac{\alpha_t}{\omega + \alpha_t}\right)^{N-R} \tag{22}$$

Therefore, assuming that the cell under investigation is from clear background, the false alarm probability has a formula given by Eq.(20). As the window sweeps over the range samples, more cells from clutter background enter into the reference set. When the cell under test comes from clutter background, the probability of false alarm takes the same form as that given by Eq.(20) after replacing $\alpha_t$ by $\alpha_c$. Since the background cells and those belonging to clutter are assumed to be independent, the CA noise level estimate has a CF of the form

$$\Omega_{Z_{CA}}(\omega) = \left(\frac{\alpha_c}{\omega + \alpha_c}\right)^R \left(\frac{\alpha_t}{\omega + \alpha_t}\right)^{N-R} \tag{23}$$

Once the CF of the noise level estimate is calculated, the computation of the processor performance becomes an easy task taking into account that the CDF of $Z_{CA}$ has a Laplace transformation given by [12].

$$\Psi_{F_z}(\omega) = \Omega_{Z_{CA}}(\omega) / \omega \tag{24}$$

### b) Ordered-Statistics (OS) Processor

OS is a CFAR technique with special immunity to interfering targets. Generally, the CFAR technique suffers some detection loss due to the adaptive threshold concept. Additionally, the presence of strong returns among the elements of the reference channel leads to an increase in the threshold, and therefore an increase in the required signal strength of the desired target. This is in effect an additional detection loss. OS-CFAR is a detection technique in which the threshold is just a scalar times one of the ranked reference cells. This concept provides inherent protection against a drastic drop in performance in the presence of spurious targets. The presence of these extraneous targets causes only gradual detection loss in the detection performance of OS scheme. In this type of CFAR schemes, the reference cells are ranked according to their input level in such a way that:

$$Y_{(1)} \le Y_{(2)} \le \ldots\ldots\ldots\ldots \le Y_{(K-1)} \le Y_{(K)} \le Y_{(K+1)} \le \ldots\ldots\ldots\ldots \le Y_{(N)} \tag{25}$$

The variable K is the rank of the cell whose input is selected to determine the detection threshold**.** In other words, the OS processor estimates the noise power simply by selecting the K<u>th</u> largest cell in the reference channel of size N. Thus,

$$Z_{OS} = Y_{(K)} \qquad \& \qquad K \in [1\,,\,N] \tag{26}$$

It can be shown that when *z* is a random variable with a PDF *f*(z) and a distribution function F(z ) , then the Kth ranked sample (out of a total of *N* samples) has a CDF given by [7]

$$F_K^{NH}(z) = \sum_{i=K}^{N} \sum_{j=MAX(0,i-R)}^{MIN(i,N-R)} \binom{N-R}{j} \binom{R}{i-j} \left(1 - F_\zeta(z)\right)^{N-R-j} \left(1 - F_\xi(z)\right)^{R-i+j} F_\zeta^{j}(z)\; F_\xi^{i-j}(z) \tag{27}$$

With

$$F_\zeta(z) = 1 - e^{-\alpha_t z} \qquad \& \qquad F_\xi(z) = 1 - e^{-\alpha_o z} \tag{28}$$

In the above expression, $F_\zeta(.)$ represents the CDF of the reference cell that contains thermal noise only whilst $F_\xi(.)$ denotes the same thing for that cell the content of which comes from outliers. The Laplace transformation of Eq.(27) yields:

$$\Psi_K^{NH}(\omega) = \sum_{i=K}^{N} \sum_{j=MAX(0,i-R)}^{MIN(i,N-R)} \sum_{\ell=0}^{i-j} \gamma_\ell\, \Phi_j(\omega) \tag{29}$$

Where

$$\gamma_\ell \triangleq \prod_{\beta=0}^{i-j-1} (r-\beta) \Big/ \prod_{\substack{\eta=0 \\ \eta\neq\ell}}^{i-j} (\ell-\eta) \tag{30}$$

And

$$\Phi_j(\omega) \triangleq \prod_{\mu=0}^{j-1} (N-R-\mu) \Big/ \alpha_t \prod_{\nu=0}^{j} \left( \frac{\omega}{\alpha_t} + N - R - \nu \right) \tag{31}$$

As we have previously shown, once the ω-domain representation of the noise level estimate is obtained, the processor performance can be easily evaluated as Eqs.(18 & 20) reveal.

### c) Trimmed-Mean (TM) Procedure

A generalization of the OS-CFAR scheme, in which the noise power is estimated by a linear combination of the ordered range samples, is the so-called trimmed-mean (TM) algorithm. The linear combination may be awaited to give best results owing to its ability in estimating the noise power level more efficiently. This processor is based on ranking the range cells according to their magnitude and then $C_1$-1 cells from the lower end and N-$C_2$ ones from the upper end are censored before adding the rest to construct the unknown noise power level. The TM-CFAR scheme reduces to the CA- and OS-CFAR processors for specific excising values. Generally, the statistic of the underlined detector takes the form:

$$Z_{TM} = \sum_{\ell=C_1}^{C_2} Y_{(\ell)} \tag{32}$$

The OS-, CA-, and TM-CFAR schemes can be treated as special cases of the above formula according to the parameter defined in Table (1).

**Table-1.** Trimming parameter values for the well-known CFAR processors

| Parameter Algorithm | $C_1$ | $C_2$ |
|---|---|---|
| **CA** | 1 | N |
| **OS(K)** | K | K |
| **TM($T_1$, $T_2$)** | $T_1$+1 | N -$T_2$ |

A more generalized version of this detector has been proposed by El Mashade [9] to include other well-known schemes. In this modified version, the unknown noise level can be estimated via

$$Z_{GTM} = \sum_{j=C_1}^{C_2-1} Y_{(j)} + \lambda Y_{(C_2)} \tag{33}$$

The well-known mean–level CFAR processors can be defined as a function of $C_1$, $C_2$, and λ in a correspondence to Table (2).

**Table-2.** Trimming and weighted parameter values for the well-known CFAR processors

| Parameter Algorithm | $C_1$ | $C_2$ | λ |
|---|---|---|---|
| **CA** | 1 | N | 1 |
| **OS(K)** | K | K | 1 |
| **CCA(K)** | 1 | K | 1 |
| **CML(K)** | 1 | K | N - K + 1 |
| **TM($T_1$, $T_2$)** | $T_1$+1 | N -$T_2$ | 1 |

The ordered statistics $Y_{(j)}$'s, j=1, ………, N are neither independent nor identically distributed random variables even if the original samples $Y_i$'s, i=1, ………., N are IID random variables. However, if the original samples $Y_i$'s are exponentially distributed and their contents are IID, the following transformation yields to another sequence the samples of which are independent.

$$Q_\ell = Y_{(C_1+\ell)} - Y_{(C_1+\ell-1)}\, U(\ell-1) \quad , \quad \ell = 0,1,........., C_2 - C_1 \triangleq C_t \tag{34}$$

U(.) in the above transformation symbolizes the unit step function.

To simplify the TM statistic, let us define another set of RV's as a linear combination of the current set, $Q_i$'s, through the mathematical formula:

$$V_j \triangleq \left(C_t - j\right) Q_j \quad \& \quad j \in \left[0, C_t\right] \tag{35}$$

The random variables $V_j$ 's are independent since $Q_j$ 's are independent. In terms of the new RV's $V_j$'s, the trimmed-mean noise level estimate $Z_{TM}$ takes the form:

$$Z_{TM} = \sum_{i=0}^{C_t} V_i \tag{36}$$

Since the random variables $V_i$'s are independent, the CF of $Z_{TM}$ is simply the product of the individual CF's of $V_i$'s. To find the CF of V, it is convenient to calculate the CF of Q which in turn a function of the CF of Y as Eq.(34) indicates. In terms of the Laplace transformation of the CDF of the ordered statistic $Y_{(i)}$'s, the CF of the random variable $Q_j$ can be easily obtained as [10].

$$\Omega_{Q_j}(\omega) = \begin{cases} \omega\, \Psi_{C_1}(\omega) & \text{for } j = 0 \\ \dfrac{\Psi_{C_1+j}(\omega)}{\Psi_{C_1+j-1}(\omega)} & \text{for } 0 < j \le C_t \end{cases} \tag{37}$$

In the above expression, $\Psi_n(\omega)$ denotes the Laplace transformation of the CDF associated with the nth ranked sample in the sequence $Y_i$'s which is given by Eq.(29) after replacing K by n.

The CF of the statistic $Z_{TM}$ can be obtained in terms of the CF of the random variable $V_j$ with the help of Eq.(35) which leads to:

$$\Omega_{Z_{TM}}(\omega) = \prod_{\ell=0}^{C_t} \Omega_{V_\ell}(\omega) = \prod_{\ell=0}^{C_t} \Omega_{Q_\ell}(\omega)\Big|_{\omega=(C_t-\ell)\omega} \tag{38}$$

As a function of the CF of the RV $Z_{TM}$, the Laplace transformation of its CDF can be easily obtained through the use of Eq.(24)

### d) The CATM-CFAR detector

To combine the good features of the CA- and TM-CFAR techniques in one version of this type of adaptive detectors, the CATM-CFAR scheme has been introduced. It optimizes the benefits of these CFAR detectors from different procedures according to the characteristics of clutter and present targets with the goal of maximizing the probability of detection at maintaining a constant rate of false alarm. It is realized by parallel operation of two types of CFAR detectors: CA-CFAR and TM-CFAR. Its structure is showed in Fig.(1).

In this figure, the CA-CFAR scheme and TM-CFAR technique carry out their operations simultaneously and independently but with the same scaling factor "T" of the detection threshold. They produce own mean clutter power level $Z$ using the appropriate CFAR algorithm. Next, they calculate own detection thresholds $T_{CA}$ and $T_{TM}$. After comparison with the content in cell under test "Θ", they decide about target presence independently. The finite decision about target presence is made in fusion center which is composed of one "AND" logic circuit. If the both input single decision in the fusion center are positive, the finite decision of the fusion center is presence of the target in CUT. In each other cases, finite decision is negative and target is not declared at the location which associated with the CUT. In each CFAR algorithm, the probability of false alarm should be constant. This fact is considered by CATM-CFAR also. Since single decision about target presence of CA and TM parts of the CATM detector are independent events, the probability of false alarm and the probability of detection of the developed version can be written as:

$$P_{FA_{CATM}} = P_{FA_{CA}} \; P_{FA_{TM}} \qquad \& \qquad P_{D_{CATM}} = P_{D_{CA}} \; P_{D_{TM}} \tag{39}$$

where

$$P_{FA_{CA}} = \Omega^{H}_{Z_{CA}}(\omega)\Big|_{\omega=T\alpha_t} = \left(\frac{1}{T+1}\right)^{N} \tag{40}$$

$$\begin{aligned} P_{FA_{TM}} &= \Omega^{H}_{Z_{TM}}(\omega)\Big|_{\omega=T\alpha_t} = \prod_{j=0}^{C_t} \Omega^{H}_{V_j}(\omega)\Big|_{\omega=(C_t-j)T\alpha_t} \\ &= T\alpha_t\,(C_t+1)\Psi^{H}_{C_1}\big(T\alpha_t(C_t+1)\big)\prod_{i=1}^{C_t}\frac{\Psi^{H}_{C_t+i}\big(T\alpha_t(C_t-i+1)\big)}{\Psi^{H}_{C_t+i-1}\big(T\alpha_t(C_t-i+1)\big)} \\ &= T(C_t+1)\sum_{j=C_1}^{N}\frac{\prod_{n=0}^{j-1}(N-n)}{\prod_{m=0}^{j}(T+N-m)}\prod_{i=1}^{C_t}\left\{\sum_{\ell=C_1+i}^{N}\frac{\prod_{n=0}^{\ell-1}(N-n)}{\prod_{m=0}^{\ell}(T+N-m)}\Bigg/\sum_{k=C_1+i-1}^{N}\frac{\prod_{n=0}^{k-1}(N-n)}{\prod_{m=0}^{k}(T+N-m)}\right\} \end{aligned} \tag{41}$$

$$P_{D_{CA}} = \left(\frac{\alpha_o}{T\alpha_s+\alpha_o}\right)^{r}\left(\frac{\alpha_t}{T\alpha_s+\alpha_t}\right)^{N-R} \tag{42}$$

and

$$P_{D_{TM}} = \Omega^{NH}_{Z_{TM}}(\omega)\Big|_{\omega=T\alpha_s} = \prod_{j=0}^{C_t}\Omega^{NH}_{V_j}(\omega)\Big|_{\omega=(C_t-j)T\alpha_s} \tag{43}$$

## 4. Processor Performance Assessment

In this section, we are going to display some numerical results that illustrate the effects of the processor parameters on its behavior against the abnormal conditions that may exist in its operating environment. These results are obtained with the aid of Matlab through the programming of the previous analytical formulas. The necessary data for running the achieved programs are N=24 and $P_{fa}=10^{-6}$. The handled results are partitioned into three groups: those associated with homogeneous background, those related to operation in clutter edges, and those attached to behavior in target multiplicity environment. Now, let us go to discuss the figures of each group individually to take an idea about the reaction of the CFAR schemes en face of the more dangerous situations of operation.

Fig.(2) illustrates the constant scaling factor "T", in dB, as a function of the ranking parameter "K" for a reference channel of 24 elements and a required rate of false alarm of $10^{-6}$ taking into account that the background channel is free of any abnormalities that deprive it from being ideally. Generally, it is observed that as K increases, T decreases as the displayed results show. For a given K value, it is noted that the OS technique has the highest T value whilst the CATM of symmetrical trimming needs the lowest T factor in order to attain the designed level of false alarm. The CA algorithm comes next to the OS scheme in achieving the thresholding factor "T". It is known that as the CFAR procedure requires lower T values, to satisfy a given rate of false alarm, as this CFAR technique estimates the unknown noise power level more efficiently. This means that the CA processor achieves a more efficient estimation of the noise power, given that the background environment is homogeneous, than the OS scheme. The symmetrical trimming TM(K, K) detector needs lower T values than the conventional CA technique especially for lower K values. On the other hand, the developed versions realize the requested rate of false alarm with the lowest T, relative to the processors stated here, values. This indicates that they accomplish the noise power level estimation in a more efficient manner. A big insight on the behavior of the T variation of the two developed techniques shows that there is a negligible decreasing in the case CAOS whilst a noticeable decreasing in CATM of symmetrical trimming, as the ranking parameter increases. This translates that the CATM(K, K) is the most efficient algorithm, among the underlined CFAR processors, in estimating the unknown noise power level and consequently it will give the highest detection performance as we predict. In other words, the developed CFAR versions have detection performance which is surpasses that of the CA scheme which is taken as a reference, for any CFAR processor, against which its homogeneous performance is compared. Fig.(3), which depicts the required scale factor to achieve a given level of false alarm for a reference channel of fixed size of estimation cells, confirms this conclusion. The family of curves of this scene reveals that the derived version CATM(4, 21) needs the lowest T values to guarantee a specified rate of false alarm and the second element, CAOS(18), in the same category comes next while the CA processor requires higher T values than them. On the other hand, the OS(18) achieves the top T values and the symmetrical TM(4, 21) scheme occupies the next situation from the higher T values point of view. From the displayed results of Figs.(2 & 3), it is clear that the developed versions of CFAR algorithms present more efficient techniques for estimating the unknown noise power level and consequently their detection threshold is more approach to that of the ideal detector.

The second category in the homogeneous group is concerned with the detection performance of the underlined detectors when their operating environment is ideal. Fig.(4) draws the detection probability against the strength of the primary target return, for a fixed size of reference channel and a given level of false alarm, of CA, OS, and TM procedures as well as their extended versions. As we predict, the CATM(4, 21) derived detector surpasses, in its detection performance, the CA scheme which is the king of the CFAR algorithms in its behavior against the homogeneous situation of operating environments. Additionally, the CAOS(18) version of the developed detectors gives also higher performance than the CA technique but less than that of the CATM(4, 21) extended processor. On the other hand, the conventional TM(4, 21) and OS(18) have detection performance which is normally worst in comparison with that of the CA algorithm. The behavior of the examined CFAR processors is a direct translation of the results obtained in the previously mentioned figures. It is of importance to note that the results of the Neymann-Pearson detector, under the same operating conditions, are included among the candidates of Fig.(4) to demonstrate to what extent the modified versions can improve the detection performance of the ordinary CFAR schemes. Fig.(5) repeats the same thing as Fig.(4) but for OS(21) and symmetrical trimmed TM(5, 20) detectors. The family of curves of this figure behaves as that of the previous figure with less degree of amelioration. As a third method to measure the enhancement of the suggested algorithms is what is called receiver operating characteristics (ROC's) in the literature of radar target detection. Fig.(6) plots the detection probability as a function of the false alarm rate at a constant level of target return for the conventional as well as derived versions along with the optimum detector which is included for the purposes of comparison. The results of the underlined figure demonstrate the previously concluded remarks which are associated with the behavior of the tested processors against the final decision about the presence or absence of the searched target. The family of curves of this figure is traced for a SNR of 10dB. A good insight on the variation of the elements of this family indicates that as the level of false alarm increases, the detection level increases also. This behavior is intuitive since increasing the false alarm rate means decreasing the detection threshold which will lead to increasing the probability of detection. The symmetrical trimming CATM(4, 21) technique gives an ROC curve which is the most closer to that of the optimum detector and CAOS(18) comes next while the conventional CA scheme occupies the third place and the ordinary symmetrically trimming TM(4, 21) scheme reserves the fourth situation before the normal OS(18) processor which has the last position among the CFAR procedures under examination. The last category of CFAR performance characterization in the underlined group is concerned with the calculation of the required signal strength to achieve a pre-assigned level of detection for a fixed size of reference channel and a given rate of false alarm. This type of performance evaluation is outlined in Fig.(7) which illustrates the needed SNR, in dB, as a function of the required probability of detection for CA, OS(18), and TM(4, 21) schemes as well as the two modified versions along with the optimum detector which is incorporated for the purpose of comparison. The curves of this family behave similarly in their variation with the desired level of detection. By examining the behavior of this category of curves, we observe that the required SNR, to obey the needed level of detection, increases as $P_d$ increases. The rate of increasing depends on the desired level of detection according to three regions of operation. In the first region, where the wanted level of detection is low, the demanded SNR increases linearly with a convenient slope. In the middle region, the rate of increasing is lower than that in the first zone and this means that the slope of the linearly increasing SNR is modest. On the other hand, the signal must be strengthened to follow up the higher demanded level of detection. This is actually the case in the third region of operation where the increasing rate of the needed SNR, to attain high wanted level of detection, becomes higher than that those in the previous two zones. The optimum detector requires the lowest SNR, the developed version CATM(4, 21) comes next, the derived scheme CAOS(18) occupies the third position, the conventional CA and TM(4, 21) algorithms reserve the fourth and fifth locations, respectively, and the last place is devoted to the OS(18) detector which needs the highest, relative the CFAR processors mentioned here, SNR to achieve a given level of detection. Generally, the two modified versions, CATM and CAOS, are good candidates of CFAR procedures that can enhance the homogeneous detection performance of the CA scheme which is the king, from the ideal detection of radar targets point of view, of this type of adaptive processors. All the scenes of the underlined group of numerical results confirm this conclusion.

If the dominant interference is clutter, rather than thermal noise or jamming, the clutter can often be highly heterogeneous. The radar may illuminate a patch of terrain that is part open field and part forested or part land and part water. When the test cell is at or near the boundary between two clutter regions having different reflectivities, the statistics in the leading and lagging subsets will not be the same. Such clutter edges can cause both false alarms at the edge and allow masking of targets in the lower reflectivity region, but near the edge. Thus, the presence of such a clutter edge may result in severe performance degradation in an adaptive threshold scheme leading to excessive false alarms or serious target masking depending upon whether the cell under test is a sample from clutter background or from relatively clear background with target return, respectively. Therefore, let us now go to discuss the figures of the second group which is concerned with the operation of the tested schemes in a background environment of clutter edges which occur when the total noise power received within a single reference window changes abruptly. The energy of interference changes in the case of the clutter edge rapidly. For example, this occurs at the border between land and sea. The set of figures of this group includes two scenes, Figs.( 8-9). Fig.(8) depicts the actual value of false alarm rate as a function of the fraction of the reference set that is immersed in clutter, in the presence of clutter edge of strength 5dB given that the detection threshold is established at a pre-request false alarm rate of $10^{-6}$, for tested detectors encompassing the new developed versions. In this situation where the transition from a clear to a clutter region is not relatively smooth, it is assumed that the total noise power density as a function of range can be represented by the step function. Two cases may be encountered in this severe clutter environment. In the first case, the cell under test is in the clear region but a group of the reference cells are immersed in the clutter. This leads to a higher adaptive threshold and the probabilities of detection and false-alarm are reduced. This is also known as the masking effect. In the second case, if the cell under test is immersed in the clutter but some of the reference cells are in the clear region, the threshold is relatively low and the probability of false-alarm is increased. Generally, jamming and the clutter edges significantly affect the power level as a function of range which results in an intolerable increase in the probability of false-alarm. As expected, $P_{fa}$ exhibits a sharp discontinuity at R=N/2. The false alarm rate of CA is superior to that of the CAOS(18) which is in turn superior to that of the CATM (4, 21) modified version. Fig.(9), which repeats the same thing as that of Fig.(8) but for a CNR of 10dB, confirms this sequence of superiority. The family of curves of this figure behaves in the same fashion as that of the previous figure within a scaling factor.

Finally, the third group of numerical results is concerned with the effect that the presence of outlying target returns amongst the candidates of reference set may cause in deteriorating the processor performance. This group incorporates two drawings, Figs.(10-11). In Fig.(10), we plot the processor detection performance in the presence of 2 and 4 spurious targets the returned signals of which are of the same strength as that of the searched target (INR=SNR). The displayed results show that, for the same number of interfering targets, the TM(4, 21) scheme has the top detection performance and OS technique comes next. The derived versions reserve the next two positions with CATM algorithm enjoys the highest priority than the CAOS procedure. The conventional CA detector has the last position in the queue of the CFAR processors. The reason of choosing 4 extraneous target returns amongst the estimation cells is to show to what extent the detection performance of the ordered statistics based detectors deteriorate when R>N-K which is the necessary condition for the OS technique to have its immunity to the presence of spurious targets. In any situation, the derived versions can enhance the heterogeneous performance of the conventional CA detector, as the results of the current figure reveal. The last scene of this group is devoted to the variation of the false alarm rate with the interference level given that there are three contaminated samples with outlying target returns among the candidates of the reference channel. Fig.(11) exposes the underlined characteristics for the tested CFAR processors to see their ability in maintaining a constant level of false alarm irrespective to the strength of the interferer's return. As shown, the conventional TM scheme represents the king of this set of adaptive detectors from the property of keeping the false alarm rate near to its designed level point of view. The OS technique reserve the second position whilst the CA detector, along with its extended versions, falls to hold the false alarm rate fixed as the interference level changes.

# 5. Conclusions

This paper deals with an improvement of the behavior of the conventional CFAR processors in detecting neighborhood targets in clutter environment. This is achieved through the combination of the well-known CA, OS, and TM procedures and developing what are named as CAOS- and CATM-CFAR schemes. A fusion of particular decisions of the internal CA- with either OS- or TM-CFAR algorithms within the CAOS- or CATM-CFAR processor provides a better final decision and detection. The advantage of using the developed versions of CFAR techniques is shown in the situation of detection of real targets in real clutter as well. Analytical expressions for the detection probability and false alarm rate for the resulting schemes are derived and their performances are compared with the performances of the original processors, from which they derived, along with the optimum detector. A set of numerical results are displayed in such a way that the role of each parameter, in controlling the behavior of the underlined CFAR processor against the variation of the operating conditions, can be demonstrated. These results show that there is an enhancement in the performance of the developed versions, relative to the conventional CA detector, either the operating environment is free of or contaminated with several outlying target returns along with the tested target. Additionally, the homogeneous reaction of the new versions outperforms that of CA technique which was taken as a reference against which the ideal performance of any CFAR processor is compared. From the interferer point of view, the multitarget performance of the derived detectors is better than that of the CA procedure but it is worst relative to that of the other one in the resulted versions; i.e. OS in the case of CAOS or TM in the situation of CATM. From the clutter edge point of view, on the other hand, the extracted detectors have minor improvement in their rate of false alarm in comparison with the CA algorithm which is taken as a reference against which the homogeneous performance of any CFAR is compared to decide it is good or worst.

# References


[1] Gandhi, P. P. and Kassam, S. A., 1988. "Analysis of cfar processors in nonhomogeneous background." *IEEE Transactions on Aerospace and Electronic Systems,* vol. 14, pp. 427-445.

[2] El Mashade, M. B., 1995. "Performance analysis of modified ordered statistics CFAR processors in nonhomogeneous environments." *Signal Processing ELSEVIER,* vol. 41, pp. 379-389.

[3] El Mashade, M. B., 1996. "Monopulse detection analysis of the trimmed mean level CFAR processor in nonhomogeneous situations." *IEE Radar, Sonar Navig,* vol. 143, pp. 87-94.

[4] El Mashade, M. B., 1998. "Detection analysis of linearly combined order statistic CFAR algorithms in nonhomogeneous background environments." *Signal Processing ELSEVIER,* vol. 68, pp. 59-71.

[5] El Mashade, M. B., 2005. "M-Sweeps exact performance analysis of OS modified versions in nonhomogeneous environments." *IEICE Trans. Commun,* vol. E88-B, pp. 2918-2927.

[6] El Mashade, M. B., 2006. "Analysis of cell-averaging based detectors for $\chi 2$ fluctuating targets in multitarget environments." *Journal of Electronics (China),* vol. 23, pp. 853-863.

[7] El Mashade, M. B., 2008. "Performance analysis of os structure of cfar detectors in fluctuating target environments." *Progress In Electromagnetics Research C,* vol. 2, pp. 127-158.

[8] Magaz1, B., Belouchrani1, A., and Hamadouche, M., 2011. "A new adaptive linear combined CFAR detector in presence of interfering targets." *Progress In Electromagnetics Research B,* vol. 34, pp. 367-387.

[9] El Mashade, M. B., 2011. "Analysis of adaptive detection of moderately fluctuating radar targets in target multiplicity environments." *Journal of the Franklin Institute,* vol. 348, pp. 941–972.

[10] El Mashade, M. B., 2012. "Performance analysis of cfar detection of fluctuating radar targets in nonideal operating environments." *American Journal of Signal Processing,* vol. 2, pp. 98-112.

[11] Wang, W. Q., 2013. *Radar Systems: Technology, principals and applications*: Nova Science Publishers, Inc.

[12] El Mashade, M. B., 2013. "Analytical performance evaluation of adaptive detection of fluctuating radar targets." *Radioelectronics and Communications Systems,* vol. 56, pp. 321–334.

[13] Dejan, I., Milenko, A., and Bojan, Z., 2014. "A new model of cfar detector." *Frequenz,* vol. 68, pp. 125–136.

[14] El Mashade, M. B., 2014. "Performance enhancement of the conventional cfar processors in ideal and multitarget environments." *Radioelectronics and Communications Systems,* vol. 57, pp. 287–305.

[15] Dejan, I., Milenko, A., and Bojan, Z., 2014. "False alarm analysis of the catm-cfar in presence of clutter edge." *Radioengineering,* vol. 23, pp. 66-72.

**Fig-1.** Architecture of CATM adaptive threshold scheme

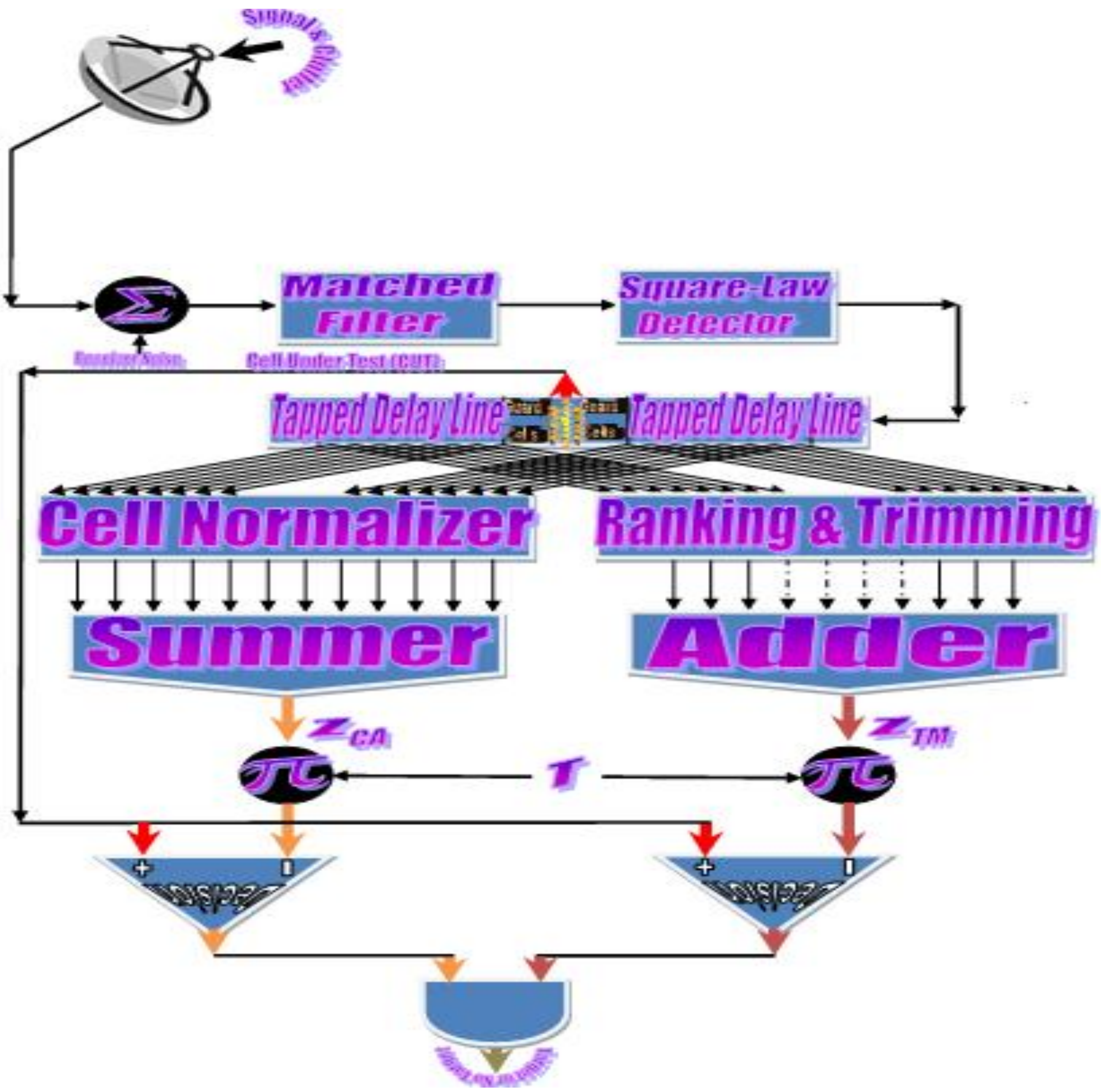


**Fig-2.** Constant scale factor (T) versus the ordering parameter (K) of the conventional, and their derived versions, CFAR schemes when N =24 and $P_{fa}=10^{-6}$.

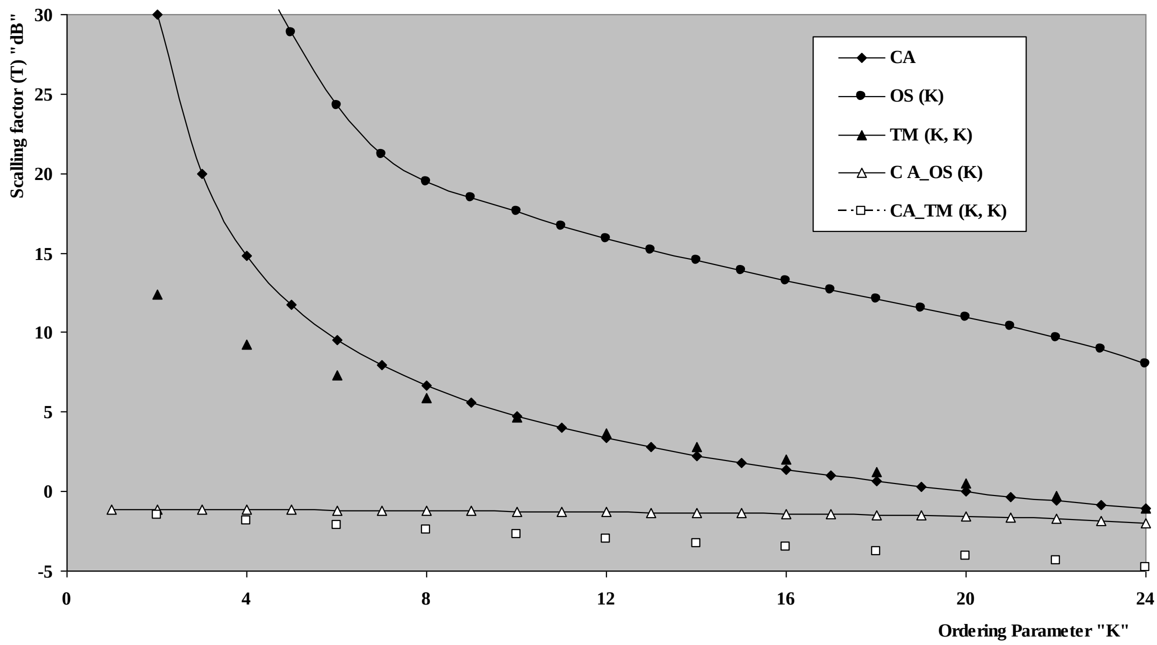

**Fig-3.** Thresholding constant (T) versus the false alarm rate (Pfa) of the conventional, as well as their developed versions, adaptive processors when the reference channel contains 24 cells.

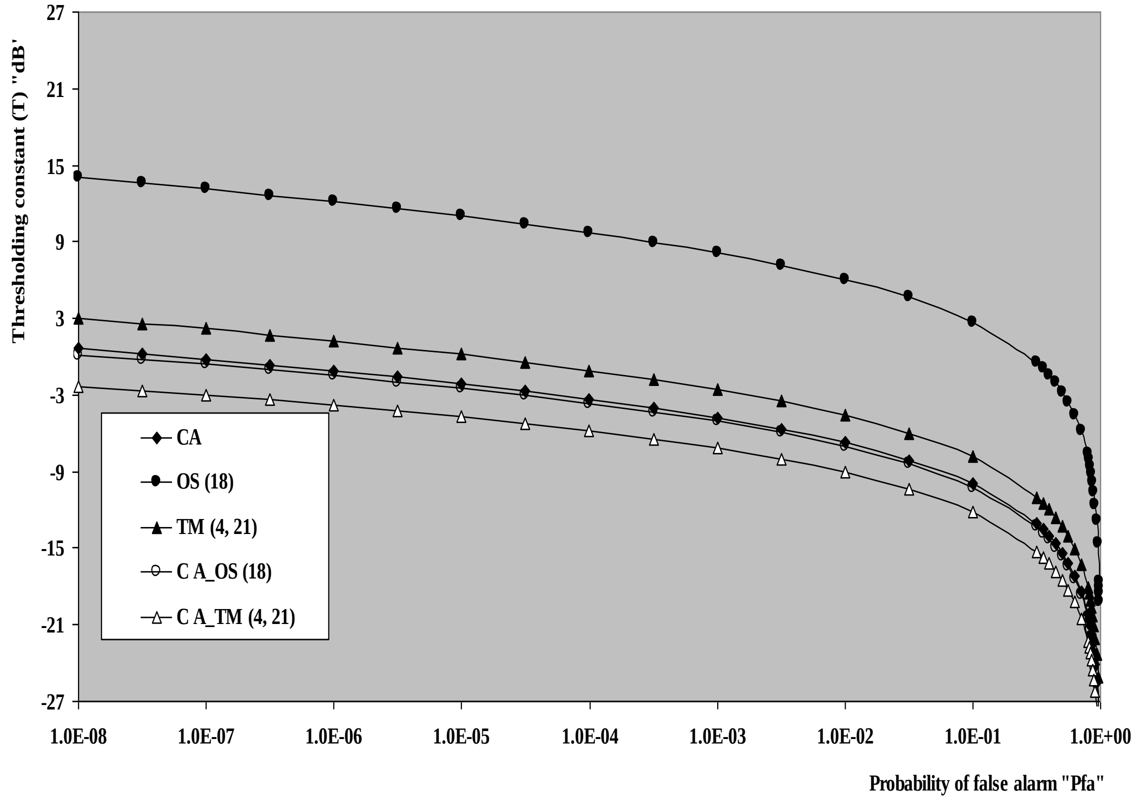


**Fig-4.** Ideal detection probability versus returned target signal strength for the conventional as well as the developed versions of CFAR processors when N=24 and Pfa=10-6.

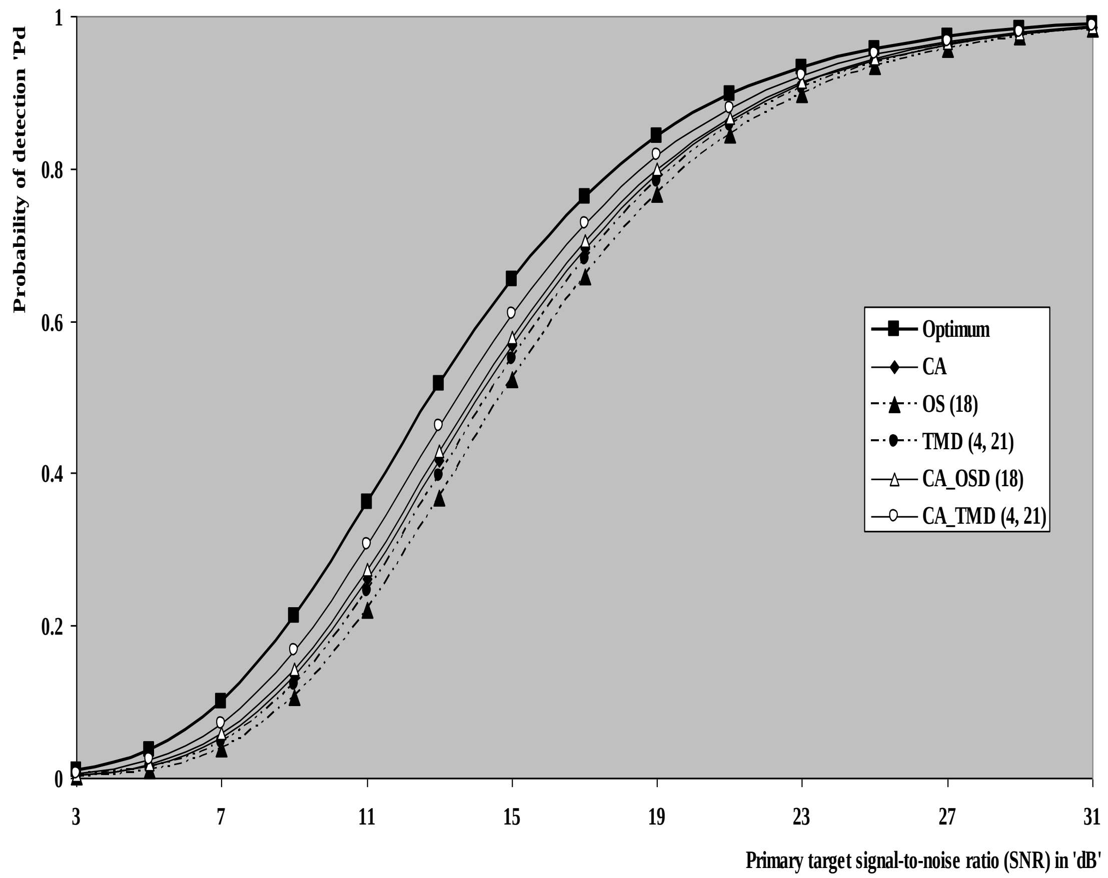

**Fig-5.** Homogeneous detection performance of the modified as well as conventional CFAR schemes when N=24 and Pfa=10-6.

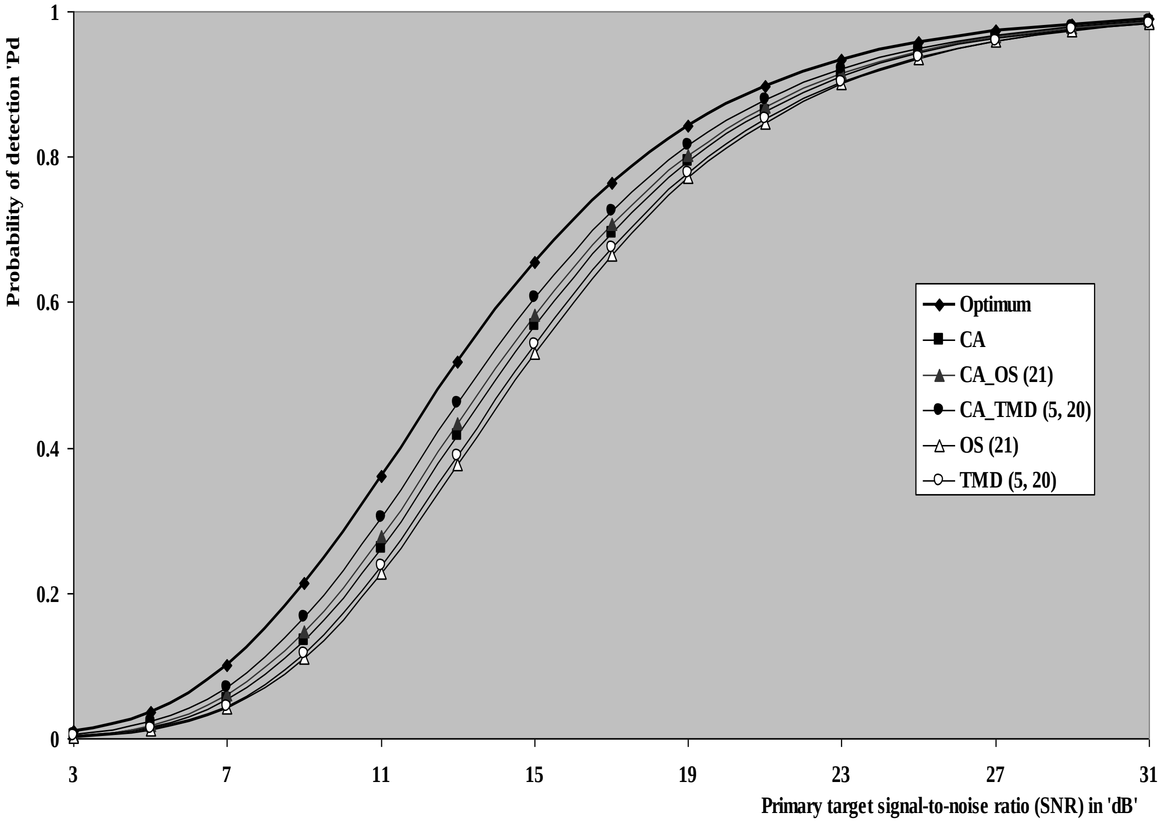


**Fig-6.** Receiver operating characteristics (ROC 's), in homogeneous situation, of conventional as well as modified versions of CFAR algorithms when N=24 and for a SNR of 10dB.

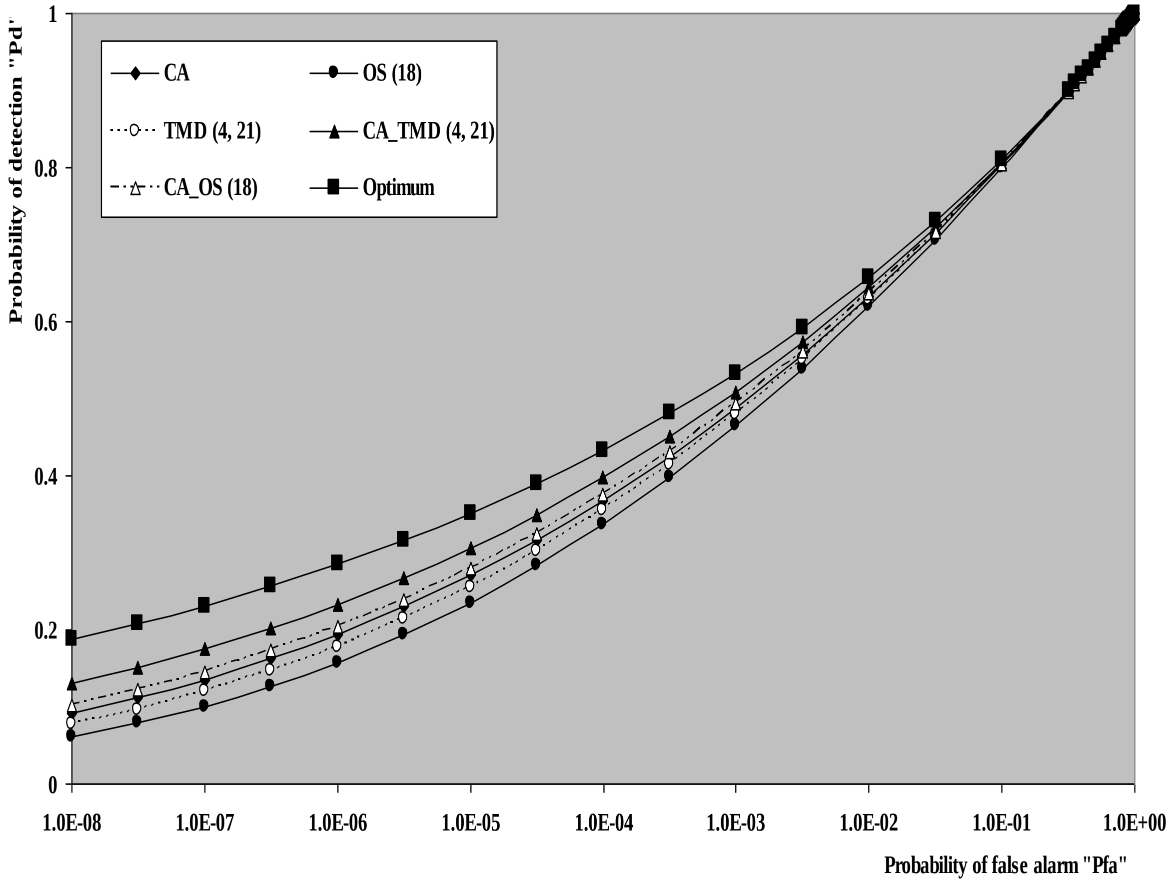

**Fig-7.** Required signal strength, in ideal background, to achieve a pre-assigned level of detection for the conventional CFAR detectors along with their developed versions when N=24 and Pfa=10-6.

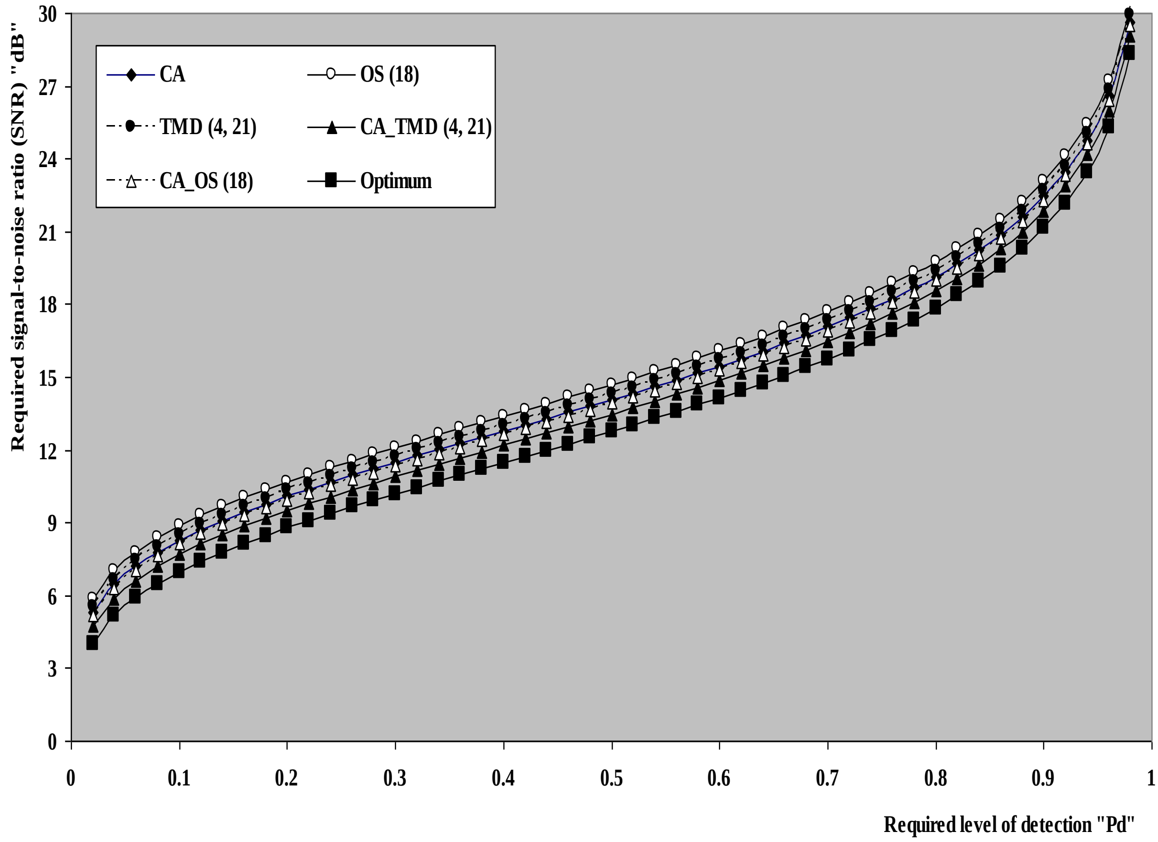


**Fig-8.** Clutter-edge false alarm rate performance of the conventional as well as derived versions of CFAR schemes for a window size of 24 cells, an edge of CNR=5dB and a designed rate of false alarm of 10-6.

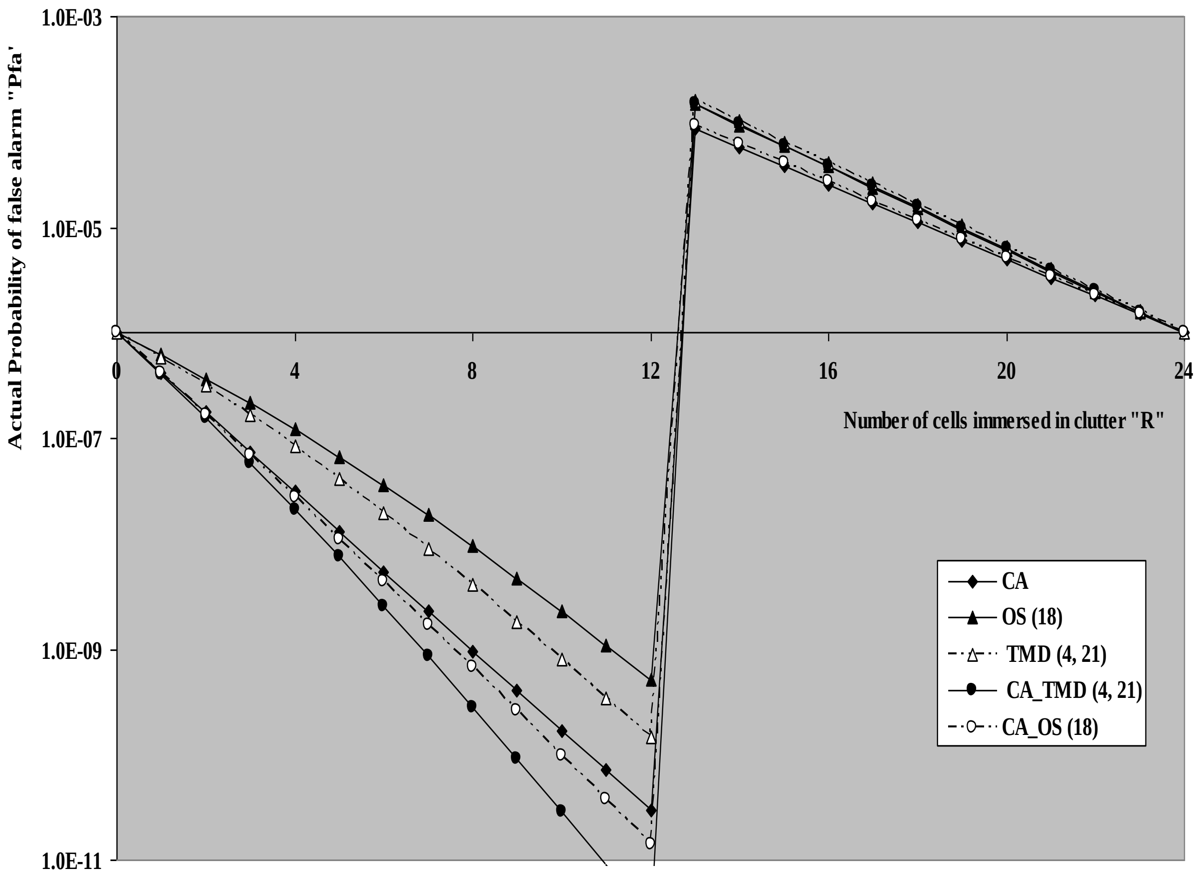

**Fig-9.** Clutter-edge false alarm rate performance of the conventional as well as modified versions of CFAR schemes for a window size of 24 cells, an edge of CNR=10dB and designed rate of false alarm of 10-6.

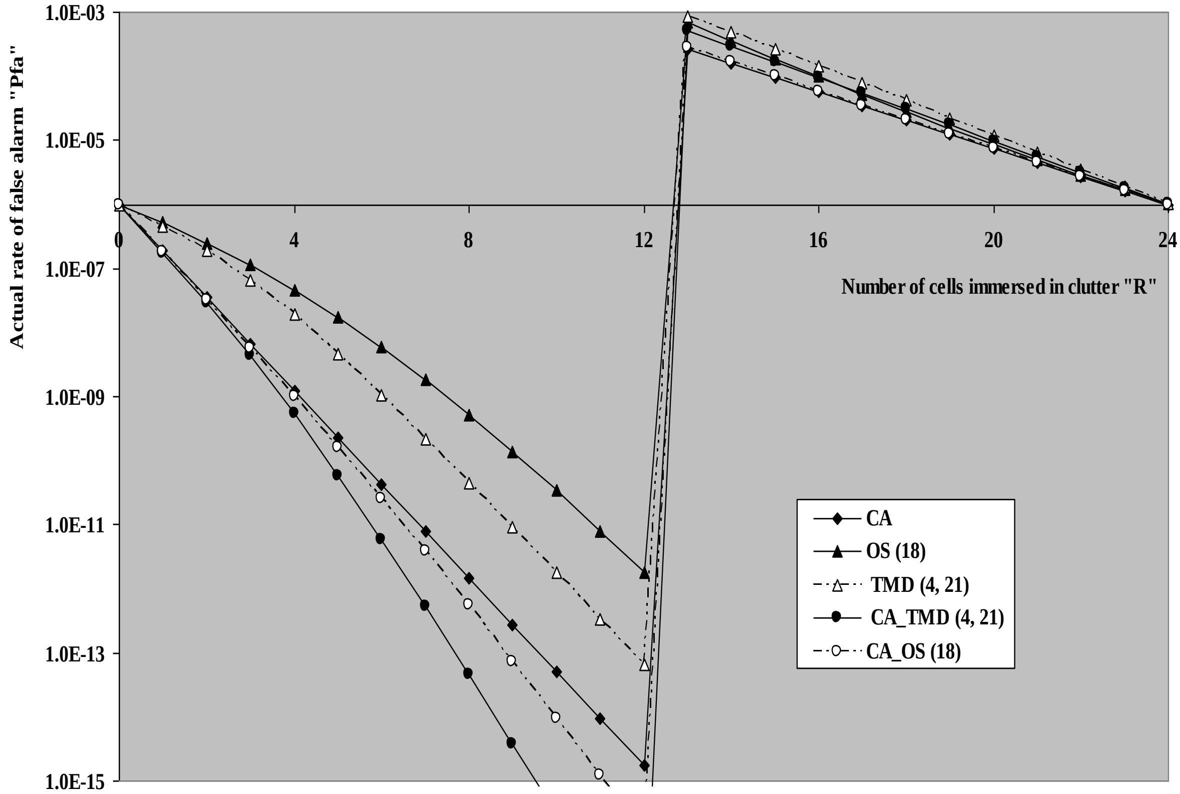


**Fig-10.** Multitarget detection performance of the conventional along with their derived versions CFAR processors for N=24, INR=SNR, and Pfa=10-6.

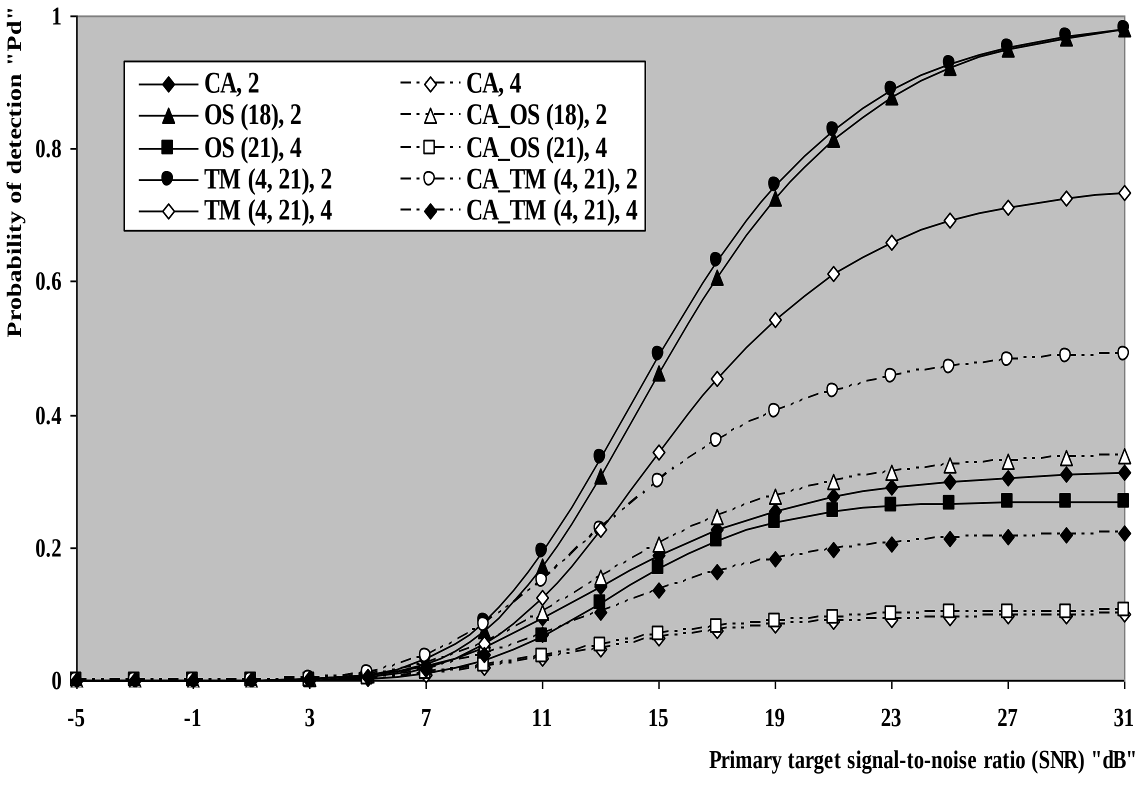

**Fig-11.** False alarm rate performance of the conventional as-well-as their developed versions of CFAR schemes in the presence of three outlying targets when N =24 and Pfa= 10-6.